388 *Biochemistry* **2011,** *50,* 388–396
DOI: 10.1021/bi101239r

BIOCHEMISTRY
including biophysical chemistry & molecular biology
Article

The Amino- and Carboxyl-Terminal Fragments of the *Bacillus thuringensis* Cyt1Aa Toxin Have Differential Roles in Toxin Oligomerization and Pore Formation†

Claudia Rodriguez-Almazan,‡ Iñigo Ruiz de Escudero,§ Pablo Emiliano Cantón,‡ Carlos Muñoz-Garay,‡ Claudia Pérez,‡ Sarjeet S. Gill,∥ Mario Soberón,‡ and Alejandra Bravo*,‡

‡*Instituto de Biotecnología, Universidad Nacional Autónoma de México, Apdo. Postal 510-3, Cuernavaca 62250, Morelos, Mexico,* §*Microbial Bioinsecticides, Instituto de Agrobiotecnología, CSIC-Universidad Publica de Navarra-Gobierno de Navarra, Mutilva Baja 31192, Spain, and* ∥*Department of Cell Biology and Neuroscience, University of California, Riverside, California 92506, United States*

Received August 3, 2010; Revised Manuscript Received December 7, 2010

ABSTRACT: The Cyt toxins produced by the bacteria *Bacillus thuringiensis* show insecticidal activity against some insects, mainly dipteran larvae, being able to kill mosquitoes and black flies. However, they also possess a general cytolytic activity in vitro, showing hemolytic activity in red blood cells. These proteins are composed of two outer layers of α-helix hairpins wrapped around a *β*-sheet. With regard to their mode of action, one model proposed that the two outer layers of α-helix hairpins swing away from the *β*-sheet, allowing insertion of *β*-strands into the membrane forming a pore after toxin oligomerization. The other model suggested a detergent-like mechanism of action of the toxin on the surface of the lipid bilayer. In this work, we cloned the N- and C-terminal domains form Cyt1Aa and analyzed their effects on Cyt1Aa toxin action. The N-terminal domain shows a dominant negative phenotype inhibiting the in vitro hemolytic activity of Cyt1Aa in red blood cells and the in vivo insecticidal activity of Cyt1Aa against *Aedes aegypti* larvae. In addition, the N-terminal region is able to induce aggregation of the Cyt1Aa toxin in solution. Finally, the C-terminal domain composed mainly of *β*-strands is able to bind to the SUV liposomes, suggesting that this region of the toxin is involved in membrane interaction. Overall, our data indicate that the two isolated domains of Cyt1Aa have different roles in toxin action. The N-terminal region is involved in toxin aggregation, while the C-terminal domain is involved in the interaction of the toxin with the lipid membrane.

Bacillus thuringiensis (Bt)[1] spore-forming bacteria produce crystalline inclusions during their sporulation phase of growth. These inclusion bodies are composed of insecticidal proteins, also known as *δ*-endotoxins that comprise two multigenic families, named Cry and Cyt (*1*). Cry toxins have been found in many Bt strains and include proteins that are toxic to different insect orders such as Lepidoptera, Diptera, Coleoptera, and Hymenoptera and to nematodes (*1*). In contrast, the Cyt toxins show dipteran specificity in vivo, being able to kill mosquitoes and black flies (*1*). However, it is possible that Cyt proteins may have an even broader spectrum of activity against insects, because other specificities of Cyt toxins have been reported; i.e., Federici and Bauer (*2*) showed that Cyt1Aa is toxic against a coleopteran larvae, the cottonwood leaf beetle (*2*). In addition to its in vivo insecticidal activity, the Cyt toxins exhibited in vitro cytolytic activity for a broad range of other cells, including erythrocytes (*1*). Cyt toxins have been most frequently found in Bt strains active against mosquitoes in combination with Cry toxins that are also specific against dipteran larvae (*1*). It was shown that combination of dipteran specific Cry proteins with Cyt induces a synergistic activity among them. Because of this synergism, their insecticidal activity is potentiated severalfold above their combined individual toxicities (*3*−*5*), and that is why they have been used extensively for mosquito control. Several insecticidal products such as Vectobac, Teknar, Bactimos, Skeetal, and Mosquito Attack are now available for the control of mosquitoes such as *Aedes aegypti* and certain *Anopheles* species that are vectors of dengue fever and malaria, respectively, or against *Simulium damnosum*, a black fly that is a vector of onchocearciasis (*6*−*8*).[1]

Cry and Cyt are pore-forming toxins, but they exhibit different three-dimensional structures and mechanisms of action. Cyt proteins are composed of a single α−*β* domain comprising two outer layers of α-helix hairpins wrapped around a *β*-sheet (*9*). The α-helices have an amphiphilic character, with the hydrophobic residues packed against the *β*-sheet. The α-helices are not long enough to span the membrane bilayer. In contrast, *β*-strands 5−7 have an estimated length that could span the width of the biological membrane (*9*).

Cry and Cyt proteins are solubilized in the gut of susceptible dipteran insects and proteolytically activated by midgut proteases (*8*, *10*). Cry toxins show a complex mechanism of action involving multiple and sequential binding interactions with specific protein receptors located in the microvilli of midgut epithelial cells (*11*, *12*). In contrast, Cyt toxins do not bind to protein receptors and directly interact with nonsaturated membrane lipids such as phosphatidylcholine, phosphatidylethanolamine, and sphingomyelin (*8*, *13*). Cyt toxin bound irreversibly to

†This research was funded in part through National Institutes of Health Grant 1R01 AI066014, Grants DGAPA/UNAM IN218608 and IN210208-N, and CONACyT Grant U48631-Q 478. I.R.d.E. received a José Castillejo postdoctoral grant and a mobility grant for teaching and research staff of Universidad Publica de Navarra-Gobierno de Navarra.

*To whom correspondence should be addressed. E-mail: bravo@ibt.unam.mx. Phone: 52 777 3291635. Fax: 52 777 3291624.

[1]Abbreviations: Cyt, cytolytic δ-endotoxin from *B. thuringiensis*; Cry, crystal δ-endotoxin from *B. thuringiensis*; Bt, *B. thuringiensis*; Bti, *Bacillus thuringiensis* subsp. *israelensis*; VVA2, cardiotoxin from *Volvariella volvacea*; SUV, small unilamellar vesicles; PC, phosphatidylcholine; Ch, cholesterol; S, stearylamine; EC_{50}, mean effective concentration; LC_{50}, mean lethal concentration; SDS−PAGE, sodium dodecyl sulfate−polyacrylamide gel electrophoresis.

 Published on Web 12/10/2010

Table 1: Sequences of Primers Used in PCR Assays

primer	sequence	restriction site
p20f	5′AAA CCC GGG TTT GAC GAG GAA ACA GAG TAT ACG AGT T3′	*Xma*I
p20r	5′TTT CCC GGG AAA TCG AAC GTC ATA TAG ATA AAA TGC3′	*Xma*I
pCytf	5′ACA AAG CTT GGC ATC TTT CGA ACT ATA GC3′	*Hin*dIII
pCytr	5′GAT GGT ACC TAT GAA AAT ATA ACG TTG3′	*Kpn*I
pNT1r	5′**CTA** AGA TTA GTA ATT TGT TTG ATT AGC AGT TTC CTT3′	none
pNT2f	5′GAA ACT GCT AAT CAA ACA AAT TAC TAA TCT **TAG**3′	none
pCT1r	5′GAC ATT GTA TGT GTA ATT TGT CAT AAA TAA ACA ACT CCT3′	none
pCT2f	5′AGG AGT TGT TTA TTT ATG_ACA AAT TAC ACA TAC3′	none

the cell membrane, inducing the formation of cation-selective channels in planar bilayers and release of radiolabeled solutes from the membrane vesicles (*14*, *15*).

There are currently two proposed models to explain the mechanism of action of Cyt toxins. One model proposed that the two outer layers of α-helix hairpins swing away from the β-sheet upon membrane contact and the long β-strands are allowed to insert into the membrane. Oligomerization proceeds, ending with the formation of a structured β-barrel pore within the membrane that kills the cells by colloid osmotic lysis (*16*). It was proposed that α-helix C−D hairpin is the hinge for the main conformational change, leaving the α-helices on the membrane surface and allowing that part of the β-sheet domain to penetrate the hydrophobic zone of the bilayer (*16*). Studies performed with synthetic peptides of Cyt1A showed that peptides corresponding to helices αA and αC are major structural elements involved in the membrane interaction and also affected the intermolecular assembly of the toxin because they were able to increase the insertion of the Cyt1Aa toxin into the membrane (*17*). Finally, the other model of the mechanism of action of Cyt toxins proposed a nonspecific aggregation of the toxin on the surface of the lipid bilayer leading to a detergent action that leads to membrane disassembly and cell death (*18*).

With regard to the molecular mechanism involved in the synergism between Cry and Cyt toxins, it was proposed that Cyt1Aa synergizes the toxic activity of Cry11Aa by functioning as a membrane-bound receptor (*19*). The specific epitopes involved in their interaction have been mapped in both toxins, and mutations in these residues severely affected their synergism (*19*). Additionally, it was shown that the binding of Cry11Aa to Cyt1Aa toxin facilitates the formation of a Cry11Aa oligomeric structure that is capable of forming pores in membrane vesicles (*20*).

Recently, it was shown that the Cyt2Ba toxin shares partial sequence similarity and a similar topological organization with volvatoxin A2 (VVA2), a pore-forming cardiotoxin from mushroom *Volvariella volvacea* (*21*). Interestingly, VVA2 is also hemolytic against red blood cells, and a functional study performed with isolated domains of VVA2 showed that the N-terminal domain, which comprised the region rich in α-helices, is responsible for the oligomerization of VVA2 in the absence of membrane lipids and inhibited the hemolytic activity of the toxin acting as a dominant negative inhibitor (*22*). In contrast, the C-terminal domain, harboring the three long β-strands, is involved in binding and insertion into the membrane (*22*).

In this work, we cloned the N- and C-terminal fragments of the Cyt1Aa toxin and analyzed their functional role. We found that like the VVA2 toxin, the N-terminal region of Cyt1Aa induced toxin aggregation in the absence of lipids and that this fragment has a dominant negative inhibitory effect on the hemolytic activity of Cyt1Aa. We also found that the N-terminal region inhibits the in vivo insecticidal activity against *A. aegypti* larvae. Finally, our data confirmed that the C-terminal domain of Cyt1Aa, a region is rich in β-strands, is involved in membrane interaction.

EXPERIMENTAL PROCEDURES

Cloning and Expression of N-Terminal and C-Terminal Fragments of Cyt1Aa. We first cloned the p20 protein gene that encodes a chaperone protein necessary for the correct folding of the Cyt1Aa protein (*23*) into the pHT315 plasmid (*24*), and then we used this construction named pHT315-p20 to clone the *cyt1Aa* gene or the two Cyt1Aa fragments. The p20 gene was amplified using total Bti DNA as a template using p20f forward and p20r reverse primers (Table 1) that contain a *Xma*I restriction site at their 5′ ends. This polymerase chain reaction (PCR) product was cloned into the unique *Xma*I site of the pHT315 plasmid to construct pHT315-p20.

The *cyt*1A gene was amplified using plasmid pWF45 (*25*) as a template and Vent-Polymerase (New England BioLabs, Beverly, MA). The primers used for this reaction, pCytf forward and pCytr reverse (Table 1), include *Hin*dIII and *Kpn*I restriction sites at their 5′ ends, respectively. This PCR product was cloned into the pHT315-p20 vector previously digested with *Hin*dIII and *Kpn*I restriction enzymes and transformed into the *B. thuringiensis* 407 acrystalliferous strain (*24*). This construction was named pHT315-cyt1Aa.

Two PCRs were performed with plasmid pWF45 as template for construction of each N-terminal or C-terminal fragments. The first PCR for the N-terminal fragment amplifies 834 bp that includes the promotor region of the *cyt1Aa* gene and the first 170 residues of the toxin (Figure 1A). This PCR was performed with pCytf forward primer and pNT1r reverse primer that includes nine nucleotides (underlined) at the 5′ end, which corresponds to a stop codon (in bold) and the beginning of the terminator region of the gene (Table 1). The second PCR for the N-terminal fragment amplifies 348 bp corresponding to the terminator region. For this PCR, we used pNT2f forward primer that completely overlaps with PNT1r and pCytr reverse primers (Figure 1A and Table 1). The PCR products were purified with the QIAquick PCR Purification Kit (QIAGEN, Valencia, CA) and used as megaprimers in a second PCR of eight cycles performed with Vent-Polymerase. Finally, pCytf and pCytr primers were added to the reaction mixture, and amplification was continued for 30 additional cycles (Figure 1A). The expected PCR product of the complete N-terminal domain was 1149 bp.

In the case of amplification of the C-terminal fragment, the first PCR amplifies 346 bp that includes the promotor region of the *cyt1Aa* gene and 21 nucleotides from the C-terminal region starting at residue 168. This PCR was performed with pCytf forward primer and pCT1r reverse primer that includes the 21

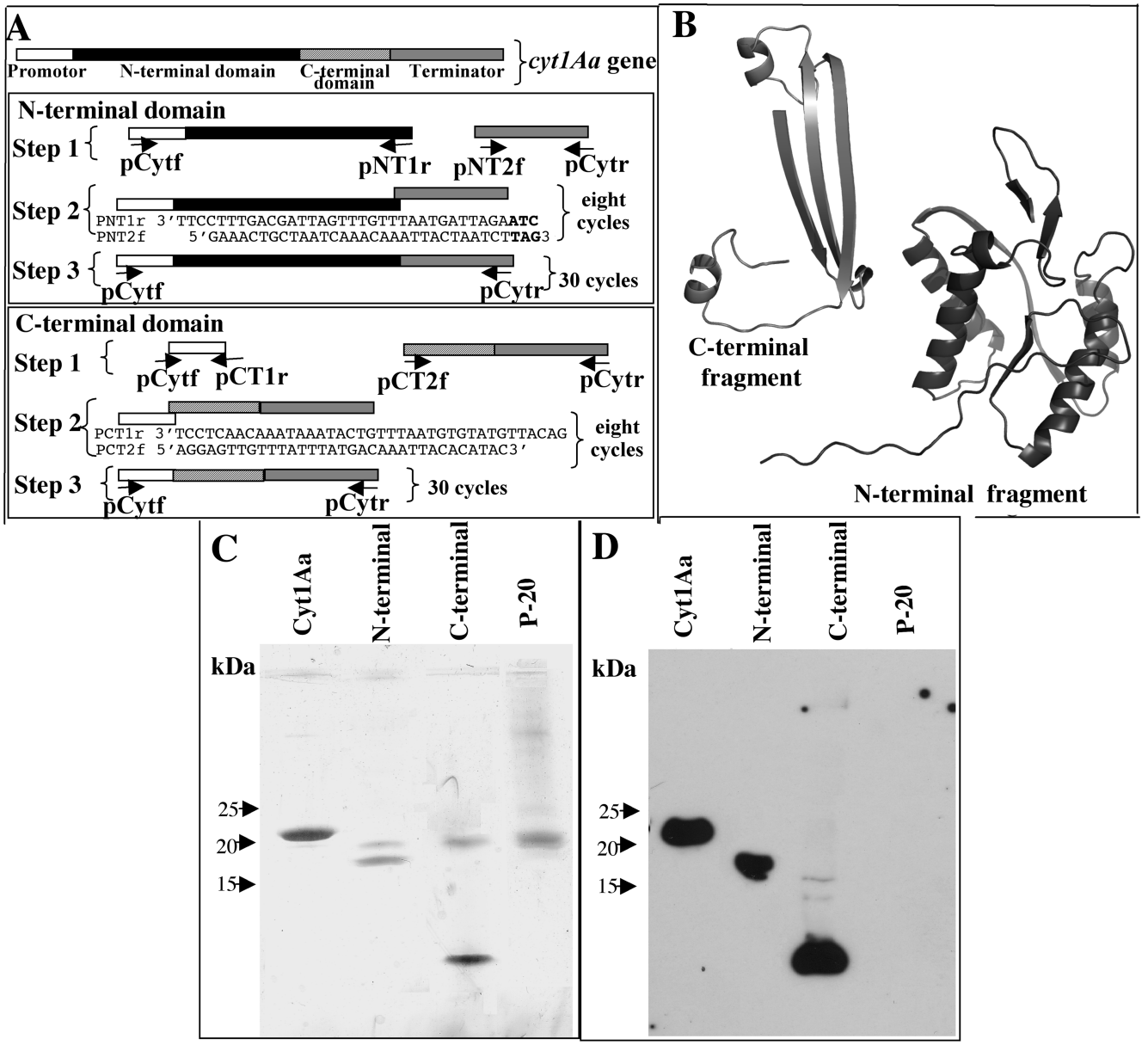

FIGURE 1: Cloning and expression of N- and C-terminal domains of Cyt1Aa toxin. (A) Schematic representation of the *cyt1Aa* gene and the PCR procedure used to amplify and finally clone each one of the two protein fragments. Sequences of primers are listed in Table 1. (B) Putative three-dimensional structure of the two Cyt1Aa fragments according to the coordinates of Cyt2Aa. (C) Silver-stained SDS−PAGE von Javow gradient gel showing that N-terminal fragment has a size of 18.9 kDa and the C-terminal fragment a size of 8.8 kDa. (D) Western blot analysis of N- and C-terminal fragments detected with a polyclonal anti-Cyt1Aa1/11 antibody and a secondary goat HRP antibody. Sizes of proteins were estimated from the molecular prestained precision plus standard, all blue (Bio-Rad).

nucleotides (underlined) mentioned above (Table 1 and Figure 1A). The second PCR for the C-terminal fragment amplifies 585 bp corresponding to the last 80 residues of Cyt1Aa (from residue 168 to 248) and the terminator region. For this reaction, we used pCT2 forward primer that overlaps completely with pCT1r and pCytr reverse primer (Table 1 and Figure 1A). These two PCR products were purified with the QIAquick PCR Purification Kit and used as megaprimers in a PCR as described above for N-terminal fragment amplification. After eight cycles of amplification, primers pCytf and pCytr were added and the reaction was continued for 30 cycles. The expected PCR product of the complete C-terminal domain was 898 bp in size. The final PCR fragments were purified with the QIAquick PCR Purification Kit and ligated bluntly into the pJET plasmid.

Both DNA constructions were first electroporated into *Escherichia coli* DH5α cells. Plasmids were purified and digested with *Hin*dIII and *Xba*I (New England BioLabs). The *Hin*dIII site was included in the PCR products, and the *Xba*I restriction site is present in the pJET plasmid. Finally, the purified digested fragments were ligated into vector pHT315-p20 previously digested with the same restriction enzymes and transformed into the *B. thuringiensis* 407 acrystalliferous strain (*24*). These constructions were named pHT315-CytNter and pHT315-CytCter, respectively.

Purification of Cyt1Aa Protein or the N-Terminal or C-Terminal Domain. Bt bacterial strains containing plasmid pHT315-Cyt1Aa, pHT315-CytNter, or pHT315-CytCter were grown at 200 rpm and 30 °C in HCT sporulation medium (*26*) supplemented with 10 μg/mL erythromycin. Spores and crystal inclusions produced by the Bt strains were harvested and washed three times with 0.3 M NaCl and 0.01 M EDTA (pH 8.0). The pellet was suspended in 0.05% Triton X-100, 300 mM NaCl, and

20 mM Tris-HCl (pH 7.2) and sonicated twice for 1 min, and inclusions were purified by sucrose gradient centrifugation (*27*). This procedure was performed twice. Protein concentrations were determined with the Bradford assay. Purified Cyt1Aa, N-terminal, and C-terminal fragment crystals were visualized via von Jagow acrylamide gradient (4 to 16%) SDS−PAGE gels (*28*) stained with silver or visualized by Western blotting as described below. Finally, these proteins were solubilized in 50 mM Na_2CO_3 and 1 mM DTT (pH 10.5). Cyt1Aa protoxin was activated with 1:30 (w/w) proteinase K (Sigma-Aldrich Co.) for 1 h at 30 °C.

Western Blot. Protein samples were boiled for 5 min in Laemmli sample loading buffer, separated via SDS−PAGE, and electrotransferred onto a PVDF membrane (Millipore, Bedford, MA). The Cyt1Aa protein or its corresponding N- or C-terminal domain was detected using the anti-Cyt1Aa1/11 polyclonal antibody (1:30000, 1 h) that was raised in rabbits against Cyt1Aa toxin and a secondary antibody coupled with horseradish peroxidase (HRP) (Sigma, St. Louis, MO) (1:5000, 1 h) followed by luminol (ECL) (Amersham Pharmacia Biotech) as described by the manufacturers. Molecular mass markers used in all SDS−PAGE runs were precision prestained plus standards, all blue (Bio-Rad).

Hemolysis Assay. Hemolytic assays were conducted as previously described (*29*). In brief, human red blood cells were diluted to a concentration of 2×10^8 cells/mL in buffer A [0.1 M dextrose, 0.07 M NaCl, 0.02 M sodium citrate, and 0.002 M citrate (pH 7.4)]. The final volume of the reaction mixture was 0.2 mL, containing 20 μL of washed blood cells, and various concentrations of Cyt1Aa in the same buffer were incubated at 37 °C for 30 min in a 96-well tissue culture plate. The supernatants were collected by centrifugation at 1290*g* for 5 min at 4 °C, and hemolytic activity was quantitated by measuring the absorbance of the supernatant at 405 nm; 100% hemolysis was defined as the same volume of human red blood cell solution incubated with dechlorinated H_2O. For analysis of inhibition of the hemolytic activity of Cyt1Aa in the presence of N-terminal or C-terminal fragments, we used mixtures with different ratios as stated in the text. The concentration of Cyt1Aa used in these hemolysis inhibition experiments was 60 ng/mL, which induced 80% hemolytic activity. These assays were conducted four times. A *t*-test made with the statistical program GraphPad Prism was used to analyze differences between observed mean values of the percentage of hemolysis induced by the toxin/fragment mixtures compared with the control (1:0 Cyt1Aa:fragment ratio). *P* values of < 0.01 (95% confidence interval) were considered statistically significant. Bars labeled with different letters indicate that differences were statistically significant.

Insect Bioassay. Mosquitocidal bioassays were performed against 20 early fourth-instar larvae in 100 mL of dechlorinated water. Ten different concentrations of purified Cyt1Aa crystals were used (50−6000 ng/mL). Positive (Bti) and negative controls (dechlorinated water) were included in the bioassay, and the viability of larvae was examined 24 h after treatment. The mean lethal concentration (LC_{50}) was estimated by Probit analysis using statistical parameters (*30*) after four independent assays (Polo-PC LeOra Software). For inhibition studies, we used a Cyt1Aa toxin concentration that kills 85% of the larvae (1.2 μg/mL) mixed with N-terminal or C-terminal domains at different Cyt1Aa:N- or C-terminal domain protein ratios (1:1, 1:0.5, and 1:0.1). A *t*-test was used to analyze differences between observed mean values of the percentage of mortality induced by the toxin/fragment mixtures compared with the control (1:0 Cyt1Aa: fragment ratio). Bars labeled with different letters indicate that differences were statistically significant.

Preparation of Small Unilamellar Vesicles (*SUV*). Egg yolk phosphatidylcholine (PC), cholesterol (Ch) (Avanti Polar Lipids, Alabaster, AL), and stearylamine (S) (Sigma) from chloroform stocks were mixed in glass vials in a 10:3:1 proportion at a 2.6 μmol final concentration and dried by argon flow evaporation followed by overnight storage under vacuum to remove residual chloroform. The lipids were hydrated in 2.6 mL of 10 mM CHES and 150 mM KCl (pH 9) by a 30 min incubation followed by vortex. To prepare SUV, we subjected the lipid suspension to sonication two times for 2 min in a Branson (Danbury, CT) model 1200 bath sonicator. SUV were used within 2−3 days of their preparation.

Oligomerization of Cyt1Aa Toxin. The oligomerization of Cyt1Aa was induced by incubation of 2 μg of Cyt1Aa-solubilized protoxin with 0.03 μmol of SUV liposomes and 0.01 μg of proteinase K for 20 min at 30 °C. A final PMSF concentration of 1 mM was added to stop the reaction. Samples were boiled for 2 min, loaded in SDS−PAGE von Jagow gradient gels, and developed by Western blotting as described above. Analysis of aggregation of Cyt1Aa was also conducted in solution in the absence of liposomes and in the presence of different ratios of N- or C-terminal fragments as described in the text.

Binding Assays and Binding Competition. The binding interaction of N- or C-terminal fragments with the SUV liposomes (0.03 μmol) was analyzed in 50 μL of binding buffer [PBS, 0.1% (w/v) BSA, and 0.05% (v/v) Tween 20 (pH 7.6)]. After incubation for 1 h at 25 °C, the membrane pellets were centrifuged at 90000 rpm for 30 min. The resulting membrane pellets or supernatants were boiled for 5 min in Laemmli sample loading buffer, loaded on SDS−PAGE gels, and transferred to Hybond-ECL nitrocellulose membranes (Amersham Biosciences). The presence of C- or N-terminal fragments in the pellet or in the supernatants was then analyzed by Western blotting.

For binding competition assays, the SUV liposomes (0.03 μmol) were incubated in 50 μL of binding buffer with 2 nM biotinylated wild-type Cyt1Aa toxin (RPN28, Amersham Biosciences) in the absence or presence of different excesses (100- or 1000-fold) of unlabeled N- or C-terminal fragments for 1 h. Unbound toxin was washed twice by centrifugation (30 min at 90000*g*). The resulting membrane pellet was boiled, loaded on SDS−PAGE gels, and transferred to nitrocellulose membranes as described above. The biotinylated toxin bound to the liposomes was visualized via incubation with the streptavidin−HRP conjugate (1:4000 dilution) for 1 h and developed with luminol as described by the manufacturers. Scanning of the 25 kDa signal was performed to quantify binding.

Fluorescence Measurements. Calcein leakage experiments were performed as described previously (*31*). Calcein-containing vesicles were prepared by sonication (two times for 2 min) of the SUV in 80 mM calcein (Molecular Probes, Eugene, OR) dissolved in 150 mM KCl and 10 mM CHES (pH 9). Non-entrapped calcein was removed by gel filtration on Sephadex G-50 (1 cm × 30 cm column) eluted with the same buffer. Calcein-loaded SUV (100 μL) were added to 900 μL of 150 mM KCl and 10 mM CHES (pH 9). Finally, samples of Cyt1Aa toxin or each of the Cyt1Aa domains were added, and the release of calcein was analyzed over time. The calcein is released because the SUV were disrupted because of the interaction of the toxin with the membrane, and then the released calcein showed an increase in fluorescence because of the dequenching of the dye into the

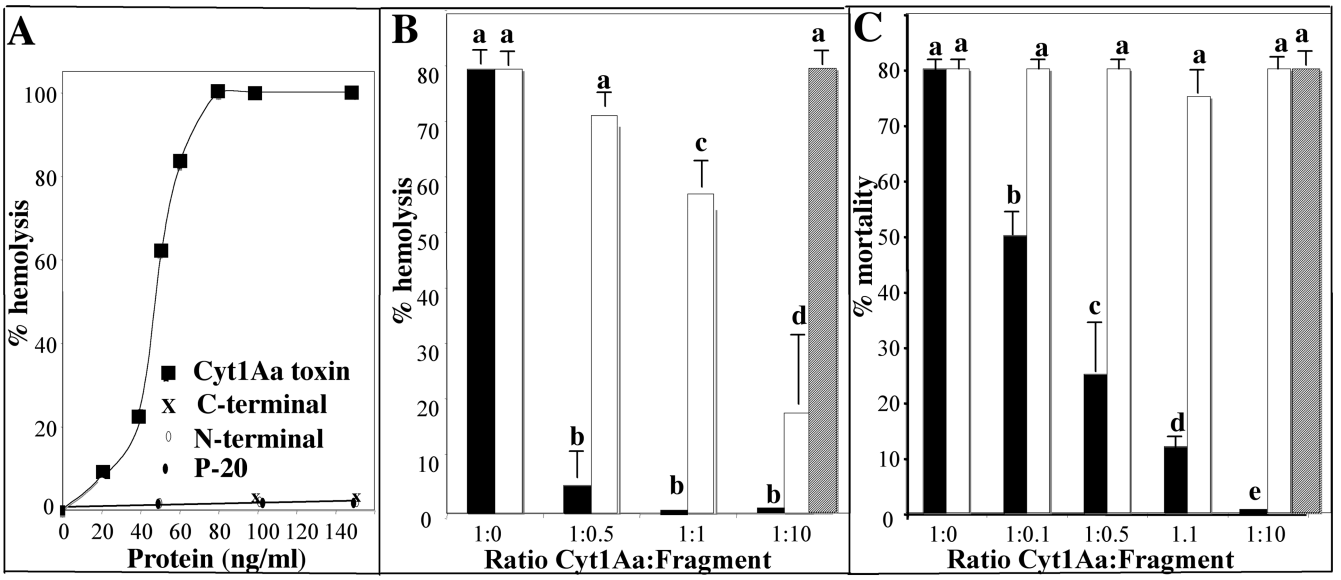

FIGURE 2: Effect of the N- and C-terminal domains of the Cyt1Aa toxin on the hemolytic activity of Cyt1Aa in red blood cells and on the in vivo insecticidal activity of Cyt1Aa against *A. aegypti* larvae. (A) Analysis of hemolytic activity of activated Cyt1Aa protein or its N- and C-terminal domains against red blood cells as described in Experimental Procedures: (■) Cyt1Aa toxin, (○) N-terminal domain, (×) C-terminal domain, and (●) P-20 protein. (B) Analysis of the effect of N- and C-terminal fragments at different molar ratios on Cyt1Aa hemolytic activity. The fragments were premixed with a Cyt1Aa protein concentration that gave 80% hemolytic activity (60 ng/mL). (C) Analysis of the effect of N- and C-terminal fragments at different molar ratios on Cyt1Aa insecticidal activity against *A. aegypti* larvae. The fragments were premixed with a Cyt1Aa protein concentration that kills 80% of the larvae (1.2 μg/mL). Each value in panel B and C represents the mean ± standard deviation of four independent experiments. A *t*-test was used to analyze statistical differences of mean values of the percentage of hemolysis or the percentage of mortality induced by the toxin/fragment mixtures compared with the control (only 1:0 ratio). Bars labeled with different letters indicate that differences were statistically significant. Black bars show data for mixtures of Cyt1Aa with the N-terminal fragment, white bars data for mixtures of Cyt1Aa with the C-terminal fragment, and dashed bars data for the mixture of p20 protein with Cyt1Aa.

external medium. Calcein fluorescence was excited at 490 nm (10 nm slit) and monitored at 520 nm with an Aminco Bowman (Urbana, IL) luminescence spectrometer. Maximal leakage at the end of each experiment was assessed by lysis with 0.1% Triton X-100 (final concentration). All fluorescence experiments were performed in triplicate at 25 °C. A *t*-test was used to analyze differences between the observed mean values of the percentage of calcein released by different concentrations of Cyt1Aa or the toxin fragments when compared with the control (No-toxin). Bars labeled with different letters indicate that differences were statistically significant.

RESULTS

Role of N- and C-Terminal Fragments in Cyt1Aa Toxin Activity. The N- and C-terminal fragments of Cyt1Aa were cloned separately into pHT315, and these new constructions were named pHT315-CytNter and pHT315-CytCter, respectively. Both of these protein fragments were expressed separately in the *B. thurngiensis* 407 strain, and crystal inclusions were purified. Figure 1A shows the schematic diagram of the PCR amplification strategy of the two fragments, and Figure 1B shows the putative three-dimensional structure of the two Cyt1Aa fragments according to the described coordinates of Cyt2Aa. The N-terminal fragment produces a protein of 18.9 kDa, and the C-terminal fragment produces a protein of 8.8 kDa. Figure 1C shows a silver-stained von Jagow SDS−PAGE gradient gel and Figure 1D the Western blot detection of the two Cyt1Aa fragments produced in Bt cells.

The hemolytic activity of activated Cyt1Aa against red blood cells was analyzed showing a medium effective concentration (EC_{50}) value of 48 ng/mL (Figure 2A). The two Cyt1Aa fragments or the p20 protein was inactive, and the mixture of N- and C-terminal fragments was also unable to induce hemolysis.

We then analyzed the effect of N- and C-terminal fragments on Cyt1Aa hemolytic activity. Different molar ratios of the N- and C-terminal fragments were premixed with a Cyt1Aa protein concentration that gave 80% hemolytic activity (60 ng/mL) as indicated in Figure 2B, and the percentage of hemolytic activity of Cyt1Aa was determined. Each value represents the mean ± standard deviation (SD) of four independent experiments. The N-terminal fragment inhibited >93% of Cyt1Aa hemolysis at 1:0.5 and 1:1 ratios. In contrast, the C-terminal fragment showed a much weaker inhibition of Cyt1Aa hemolysis because at a 1:0.5 ratio the inhibition of hemolysis of Cyt1Aa was not statistically significant ($P = 0.1002$). At a 1:1 ratio, the C-terminal fragment inhibited only 27% of the total hemolytic activity ($P = 0.0009$), and only at a 1:10 ratio did we observe a clear 75% inhibition of total Cyt1Aa hemolytic activity ($P = 0.0001$). Finally, the control performed with p20 protein at a 1:10 ratio did not affect the hemolytic activity of Cyt1Aa (Figure 2B).

The toxicity of the Cyt1Aa protoxin was also analyzed in bioassays by feeding a Cyt1Aa crystal suspension to fourth-instar *A. aegypti* larvae. The medium lethal concentration was 660 ng/mL (from 463 to 929 ng/mL, 95% confidence limit). In contrast, the N- and C-terminal fragments and the p20 protein were completely inactive when tested individually in bioassays against *A. aegypti* at 10 μg/mL. We then analyzed the effect of these fragments on Cyt1Aa toxicity, using a toxin concentration that kills 80% of the larvae (1.2 μg/mL) mixed with different molar ratios of purified crystals from the N- or C-terminal fragment. The N-terminal fragment was highly effective in blocking insecticidal activity because at a 1:0.5 or 1:1 ratio the N-terminal fragment was able to inhibit >70% of the insecticidal activity of

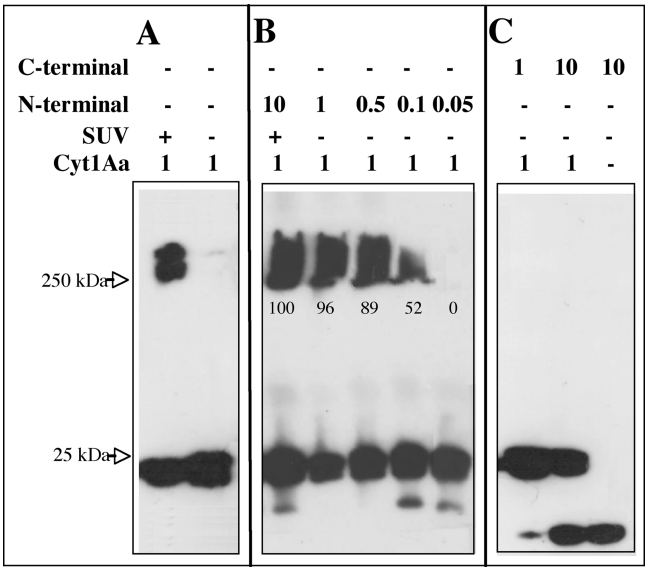

FIGURE 3: Analysis of formation of Cyt1Aa oligomers by Western blotting using polyclonal anti-Cyt1Aa/11 antibody and a secondary goat HRP antibody. (A) Cyt1Aa protoxin was activated with proteinase K in the presence or absence of SUV (PC/Ch/S mixture) liposomes. (B) Analysis of the effect of the N-terminal fragment at different molar ratios on oligomerization of Cyt1Aa in the absence of lipid membranes. The N-terminal fragment triggers aggregation of Cyt1Aa in the absence of lipid membranes. (C) Analysis of the effect of the C-terminal fragment at different molar ratios on the oligomerization of Cyt1Aa in the absence of lipid membranes. The sizes of proteins were estimated from molecular prestained precision plus standard, all blue (Bio-Rad). Numbers within the images represent the percentages of the aggregate that was formed in the presence of the N-terminal fragment as determined by scanning optical density of bands in the blots.

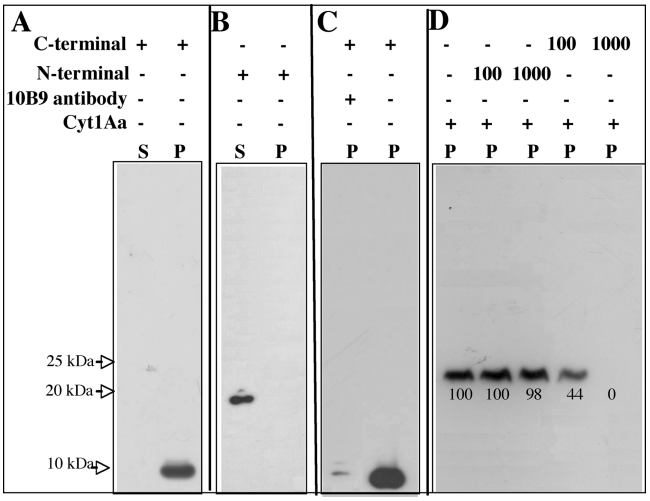

FIGURE 4: Analysis of the interaction of N-terminal or C-terminal fragments with the membrane. (A) The C-terminal fragment was incubated with SUV (PC/Ch/S mixture), and then the membrane fraction was separated by centrifugation at 90000 rpm for 30 min and visualized by Western blotting using a polyclonal anti-Cyt1Aa/11 antibody and a secondary goat HRP antibody. (B) Interaction of the N-terminal fragment with SUV (conditions identical to those described for panel A). (C) Effect of monoclonal antibody 10B9 at a 3:1 molar ratio (10B9:Cyt1Aa) on the binding of the C-terminal fragment to SUV liposomes. The presence of the C-terminal fragment bound to the membrane was visualized by Western blotting as described for panel A. (D) Binding competition assay analyzing the binding of the biotin-labeled Cyt1Aa toxin to SUV liposomes in the presence of a 100- or 1000-fold molar excess of unlabeled C- or N-terminal fragments. The bioninylated toxin was visualized with a streptavidin−HRP conjugate. The scanning optical density of the 25 kDa bands in the blot was determined to quantify binding. The sizes of proteins were estimated from molecular prestained precision plus standard, all blue (Bio-Rad). Here S denotes supernatant and P membrane pellet.

the Cyt1Aa toxin in vivo (P = 0.0001). In contrast to the C-terminal fragment or the p20 protein that did not inhibit the toxicity of the Cyt1Aa toxin even at a 1:10 ratio (Figure 2C), a P value of 1 indicates that differences in these assays were not statistically significant.

Oligomerization of Cyt1A. It was previously shown that Cyt1Aa protein was able to from large aggregates that migrated as a high-molecular mass band via SDS−PAGE after interaction with liposomes or with different cells (*32*). The aggregate is shown to be highly stable under the denaturant conditions of SDS−PAGE gels where the sample is boiled and was also analyzed via gradient centrifugation (*32*). We analyzed the aggregation of the Cyt1Aa toxin after its interaction with SUV liposomes prepared with a 10:3:1 PC/Ch/S mixture as described in Experimental Procedures. We incubated the Cyt1Aa protoxin in the presence of SUV liposomes and proteinase K and observed the formation of a similar high-molecular mass aggregate as previously described (*32*). This aggregate was also similar to the high-molecular mass aggregate observed when VVA2 interacts with lipid membranes (*22*) (Figure 3A). The observed band at the high molecular mass shows a diffuse pattern; this could be due to a heterogeneous aggregate of monomers, or aggregates may have a more hydrophobic structure that has been observed for the 250 kDa oligomers of Cry toxins (*12*). It is, however, quite important to note that in the absence of SUV the Cyt1Aa toxin was unable to form any kind of aggregate structure and remains monomeric (Figure 3A).

The aggregation of Cyt1Aa was then analyzed in the absence of SUV liposomes when different ratios of N- or C-terminal fragments were present in the assay. The N-terminal fragment induced the formation of a high-molecular mass band similar to that observed in the presence of lipid membranes described above, suggesting that this fragment induced aggregation of Cyt1Aa in solution. The aggregation of Cyt1Aa was observed at very low concentrations of the N-terminal fragment (1:0.1 Cyt1Aa:N-terminal fragment ratio) (Figure 3B). In contrast, the C-terminal fragment did not induce aggregation of Cyt1Aa in solution in the absence of SUV, even at a high concentration (1:10 ratio).

Interaction of N- and C-Terminal Fragments with the Membrane. The binding interaction of N- or C-terminal fragments with the membrane was analyzed after incubation for 1 h with SUV. Figure 4A shows that the C-terminal fragment was associated with the membrane pellet. In contrast, the N-terminal fragment did not associate with the membrane and remained in solution (Figure 4B).

It was previously reported that monoclonal antibody 10B9 that recognized the native form of the Cyt1Aa toxin inhibits 92% of the binding of the toxin to Cf1 cells from *Choristoneura fumiferana*, when used at 3:1 molar ratio (10B9:Cyt1Aa) (*32*). We analyzed whether the interaction of the C-terminal fragment with the SUV liposome domain could also be blocked by the 10B9 antibody. Figure 4C shows that the 10B9 antibody inhibited the toxin binding to the membrane pellet, suggesting that this C-terminal toxin fragment is interacting with the membrane in a similar way as the complete Cyt1Aa protein. In addition, we

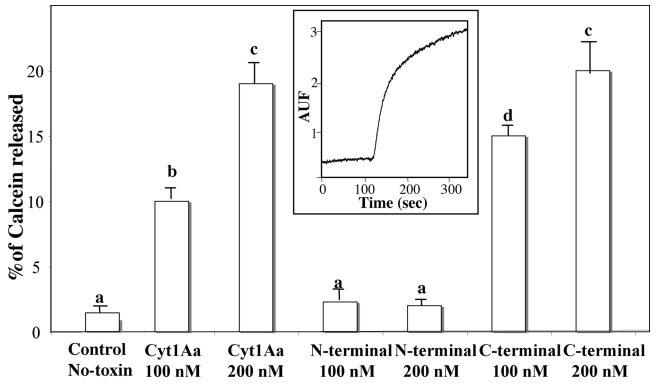

FIGURE 5: Analysis of pore formation activity of Cyt1Aa and its N- and C-terminal fragments using a calcein leakage assay. Calcein-loaded SUV (PC/Ch/S mixture) suspended in 150 mM KCl and 10 mM CHES (pH 9) were incubated with the different protein samples at two concentrations, and the release of calcein was analyzed. Maximal leakage at the end of each experiment was assessed with 0.1% Triton X-100. Each value represents the mean ± SD of three independent experiments. A *t*-test was used to analyze statistical differences of mean values of the percentage of calcein released by different concentrations of Cyt1Aa or the toxin fragments when compared with the control (No-toxin). Bars labeled with different letters indicate that differences were statistically significant. The inset shows a representative trace of the calcein release assay performed with the Cyt1Aa toxin.

performed binding competition assays analyzing the binding of the biotin-labeled Cyt1Aa toxin to SUV liposomes in the presence of a 100- or 1000-fold molar excess of C- or N-terminal fragments. Figure 4D shows that only the C-terminal fragment was able to affect the interaction of the toxin with the SUV liposomes. All these data support the hypothesis that the C-terminal region has a role in membrane interaction.

Finally, to confirm that the C-terminal fragment was able to interact with the membrane, we analyzed whether this protein fragment was able to form pores or affect the integrity of membrane liposomes. The integrity of lipid membrane vesicles was analyzed using calcein release assays. The release of entrapped calcein from SUV was measured as dequenching of the calcein fluorescence and was thereby monitored continuously as an increase in the fluorescence intensity. Data are expressed as the percentage of the maximal fluorescence release, obtained with the positive control Triton X-100. The inset in Figure 5 shows a representative trace showing that Cyt1Aa induces a fast release of encapsulated calcein. A similar fast release of calcein was induced with the soluble C-terminal fragment at 200 nM with a *P* value of 0.5992 that indicated that differences were not statistically significant from the result obtained with the wild-type toxin at the same concentration. In contrast, the N-terminal fragment was unable to affect the membrane integrity and did not release the entrapped calcein fluorophore. Calcein release is an indirect assay, and these data clearly indicated that the C-terminal fragment is able to affect the integrity of the SUV liposomes. However, the exact mechanism of C-terminal action in the membrane still remains to be determined.

DISCUSSION

In this work, we demonstrate that the two domains of Cyt1Aa may play a different role in toxin action. Our data suggest that the N-terminal region is important for the induction of toxin aggregation, while the C-terminal domain is important for membrane binding and affects membrane permeability. Similar roles were previously described for the N- and C-terminal domains of VVA2 that shares a similar topological structure with Cyt1Aa. Overall, our data suggest that both toxins, VVA2 and Cyt1Aa, may work with a similar mechanism of action. However, it is very important to notice that they are different toxins that have different specificities of action in vivo, because Cyt1Aa is active against dipteran larvae in contrast to VVA2 that is a cardiotoxin that causes cardiac arrest by affecting accumulation of Ca^{2+} in the microsomal fraction of the sarcoplasmic reticulum of the ventricular muscle in mammals. The main difference between these two proteins is that the VVA2 toxin harbors a specificity domain composed of two extra β-strands that are absent in the Cyt1Aa protein. This region is involved in heparin binding on the cell membrane and is conserved among several cardiotoxins isolated from snake venoms. In contrast, the specificity domain of Cyt1Aa has not been clearly identified. However, Cyt1Aa is currently used worldwide in the control of mosquitoes, and fully understanding its mechanism of action is quite important.

Cyt1Aa has a high affinity for the lipids found in mosquito membranes, and it was reported previously that the interaction with lipids rapidly induces toxin aggregation. Large aggregates were observed after incubation of the Cyt1Aa toxin with synthetic membranes such as PC (*33*) or mixtures of lipids [i.e., PC/Ch/S mixture (*34*)]. The association of Cyt toxins with the membrane has also been analyzed after interaction with different cells (*32*). In the case of Cyt1Aa, it was previously shown that this protein is able to interact with Cf1 cells, from a cell line derived from *Ch. fumiferana* larvae, or with human red blood cells, inducing oligomerization (*32*). The molecular size of the oligomer was estimated in linear sucrose density gradients after incubation of the iodinated toxin with these cells. The oligomer of Cyt1Aa in Cf1 showed a size of 400 kDa, while in red blood cells its size was 170 kDa. The molecular size of aggregates remains constant even if higher toxin concentrations are used in the assay, suggesting an ordered oligomerization state of the toxin in each type of cell. On the basis of density gradient centrifugation analysis, it was proposed that Cyt1Aa forms high-molecular mass oligomers in insect cells composed of 16 monomer molecules (*32*). In another report, the association of Cyt2Aa with red blood cells was studied at different temperatures, showing that rate of pore formation was low at low temperatures, suggesting that low temperatures did not inhibit binding of the toxin to the membrane but markedly slowed oligomerization. It was proposed that the Cyt2Aa toxin inserts into the membrane before oligomerization and then oligomerization of the toxin results in pore formation (*35*).

In this work, we show that the Cyt1Aa toxin is able to form high-molecular mass structures after incubation with the SUV liposomes (PC/Ch/S). In contrast, in solution the toxin remains in its monomer state. We found that the N-terminal fragment was able to trigger aggregation of the toxin in solution, forming aggregates similar in size to those found when Cyt1Aa interacts with membrane lipids. The N-terminal fragment was also able to completely inhibit the hemolytic activity of the toxin in vitro and the in vivo insecticidal activity in mosquito larvae, showing a dominant negative phenotype. These results may suggest that the aggregate formed in the presence of the N-terminal fragment is inactive. However, this remains to be demonstrated. Recently, it was reported that A61C and S108C mutants isolated in the closely related Cyt2Aa toxin, located in helices α-A and α-C, respectively, did not form oligomeric structures after incubation with membrane liposomes. These mutants were severely affected

in their hemolytic activity (*36*), supporting the hypothesis that these regions of Cyt toxins may have an important role in toxin action and that toxin oligomerization is a necessary step for toxin action. In another report, the authors analyzed the interaction of Cyt1Aa labeled with a fluorescent dye with PC liposomes. They reported that labeled Cyt1Aa strengthened its interaction with the membrane if unlabeled toxin was added to the assay, suggesting that oligomerization of several monomers of the toxin increased its capacity to interact with the membrane. They also showed that unlabeled synthetic peptides corresponding to helices αA and αC strengthened the interaction of labeled Cyt1Aa with the liposomes, suggesting that these regions of the toxin may serve as the structural seeding elements that trigger the oligomerization process of Cyt1Aa (*17*).

Our results also showed that the C-terminal domain is involved in interaction and insertion into the membrane. These data correlated with a previous study that showed that the C-terminal region of the toxin was inserted into the membrane, whereas the N-terminal region of the toxin could be removed when the membrane-bound Cyt1Aa toxin was treated with proteases (*34*). In addition, fluorescence spectroscopy analysis of selected mutant proteins of Cyt1Aa, which were labeled with the polarity sensitive dye acrylodan, showed that strands β5, β6, and β7 insert into the membrane (*16*). The authors suggested that the pores formed by the Cyt1Aa toxin are assembled from the three major β-strands present in the C-terminal half of the toxin (*16*).

Finally, different data support the possibility that a structured pore inserted into the membrane is involved in the mechanism of action of Cyt1Aa. In the first place, Cyt1Aa forms ion channels when analyzed in planar lipid bilayers (*14*), and these data were supported by studies of the dissipation of diffusion potential as a measurement of toxin pore formation activity (*17*). Cyt1Aa was more potent in permeating large unilamellar vesicles than SUV, indicating that the toxin forms pores in the membrane rather than acting as a detergent (*17*). In this work, we reported that the isolated C-terminal fragment was capable of inducing calcein release in vitro while it lacked biological activity. These observations could suggest that the function of the N-terminal domain in triggering oligomerization of Cyt1Aa is required for in vivo toxicity against mosquito larvae and that the in vitro pore formation activity of the C-terminal fragment may result from a nonspecific destruction of the membrane integrity that remains to be analyzed. It is also possible that the C-terminal fragment may be degraded in the highly proteolytical environment of the midgut lumen of the larvae, explaining its lack of activity in vivo.

In summary, the results presented here allowed us to propose that the Cyt1Aa toxin first binds the membrane as a monomer with some regions present in the C-terminal domain, and then a conformational change induced in the N-terminal domain triggers oligomerization of the toxin that leads to penetration of the β-strand present in the C-terminal domain into the lipid bilayer, resulting in membrane permeabilization.

ACKNOWLEDGMENT

We thank Lizbeth Cabrera and Jorge Arturo Yañez for technical assistance.

REFERENCES

1. de Maagd, R. A., Bravo, A., Berry, C., Crickmore, N., and Schnepf, H. E. (2003) Structure, diversity and evolution of protein toxins from spore-forming entomopathogenic bacteria. *Annu. Rev. Genet. 37*, 409–433.
2. Federici, B., and Bauer, L. S. (1998) Cyt1Aa protein of *Bacillus thuringiensis* is toxic to the cottonwood leaf beetle, *Chrysomela scripta*, and suppresses high levels of resistance to Cry3Aa. *Appl. Environ. Microbiol. 64*, 4368–4371.
3. Chilcott, C. N., and Ellar, D. J. (1988) Comparative study of *Bacillus thuringiensis* var. *israelensis* crystal proteins *in vivo* and *in vitro*. *J. Gen. Microbiol. 134*, 2551–2558.
4. Tabashnik, B. (1992) Evaluation of synergism among *Bacillus thuringiensis* toxins. *Appl. Environ. Microbiol. 58*, 3343–3346.
5. Wu, D., Johnson, J. J., and Frederici, B. A. (1994) Synergism of mosquitocidal toxicity between CytA and CryIVD proteins using inclusions produced from cloned genes of *Bacillus thuringiensis*. *Mol. Microbiol. 13*, 965–972.
6. Guillet, P., Kurstak, D. C., Philippon, B., and Meyer, R. (1990) Use of *Bacillus thuringiensis israelensis* for Onchocerciasis control in West Africa. In Bacterial control of mosquitoes and black flies (de Barjac, H., Sutherland, D. J., Eds.) pp 187, Rutgers University Press, Piscataway, NJ.
7. Becker, N. (2000) Bacterial control of vector-mosquitoes and black flies. In Entomopathogenic bacteria, from laboratory to field application (Charles, J. F., Delécluse, A., and Nielsen-LeRoux, C., Eds.) pp 383−396, Kluwer Academic Publishers, Dordrecht, The Netherlands.
8. Bravo, A., Gill, S. S., and Soberón, M. (2005) *Bacillus thuringiensis* mechanisms and use. In Comprehensive Molecular Insect Science, pp 175−206, Elsevier BV, Amsterdam.
9. Li, J., Koni, P. A., and Ellar, D. J. (1996) Structure of the mosquitocidal δ-endotoxin CytB from *Bacillus thuringiensis* sp. *kyushuensis* and implications for membrane pore formation. *J. Mol. Biol. 257*, 129–152.
10. Schnepf, E., Crickmore, N., Van Rie, J., Lereclus, D., Baum, J., Feitelson, J., Zeigler, D. R., and Dean, D. H. (1998) *Bacillus thuringiensis* and its pesticidal crystal proteins. *Microbiol. Mol. Biol. Rev. 62*, 775–806.
11. Pacheco, S., Gómez, I., Arenas, I., Saab-Rincon, G., Rodríguez-Almazán, C., Gill, S. S., Bravo, A., and Soberón, M. (2009) Domain II loop 3 of *Bacillus thuringiensis* Cry1Ab toxin is involved in a "ping pong" binding mechanism with *Manduca sexta* aminopetidase-N and cadherin receptors. *J. Biol. Chem. 284*, 32750–32757.
12. Bravo, A., Gómez, I., Conde, J., Muñoz-Garay, C., Sánchez, J., Miranda, R., Zhuang, M., Gill, S. S., and Soberón, M. (2004) Oligomerization triggers binding of a *Bacillus thuringiensis* Cry1Ab pore-forming toxin to aminopeptidase N receptor leading to insertion into membrane microdomains. *Biochim. Biophys. Acta 1667*, 38–46.
13. Thomas, W. E., and Ellar, D. J. (1983) Mechanism of action of *Bacillus thuringiensis* var *israelensis* insecticidal δ-endotoxin. *FEBS Lett. 154*, 362–368.
14. Knowles, B. H., Blatt, M. R., Tester, M., Horsnell, J. M., Carroll, J., Menestrina, G., and Ellar, D. J. (1989) A cytolytic δ-endotoxin from *Bacillus thuringiensis* forms cation-selective channels in planar lipid bilayers. *FEBS Lett. 244*, 259–262.
15. Knowles, B. H., White, P. J., Nicholls, C. N., and Ellar, D. J. (1992) A broad-spectrum cytolytic toxin from *Bacillus thuringiensis* var. *kyushuensis*. *Proc. R. Soc. London, Ser. B 248*, 1–7.
16. Promdonkoy, B., and Ellar, D. J. (2000) Membrane pore architecture of a cytolytic toxin from *Bacillus thuringiensis*. *Biochem. J. 350*, 275–282.
17. Gazit, E., Burshtein, N., Ellar, D. J., Sawter, T., and Shai, Y. (1997) *Bacillus thuringiensis* cytolytic toxin associates specifically with its synthetic helices A and C in the membrane bound state. Implications for assembly of oligomeric transmembrane pores. *Biochemistry 36*, 15546–15554.
18. Butko, P. (2003) Cytolytic toxin Cty1Aa and its mechanism of membrane damage: Data and hypotheses. *Appl. Environ. Microbiol. 69*, 2415–2422.
19. Pérez, C., Fernandez, L. E., Sun, J., Folch, J. L., Gill, S. S., Soberón, M., and Bravo, A. (2005) *Bti* Cry11Aa and Cyt1Aa toxins interactions support the synergism-model that Cyt1Aa functions as membrane-bound receptor. *Proc. Natl. Acad. Sci. U.S.A. 102*, 18303–18308.
20. Pérez, C., Muñoz-Garay, C., Portugal, L. C., Sánchez, J., Gill, S. S., Soberón, M., and Bravo, A. (2007) *Bacillus thuringiensis* subsp. *israelensis* Cyt1Aa enhances activity of Cry11Aa toxin by facilitating the formation of a pre-pore oligomeric structure. *Cell. Microbiol. 9*, 2931–2937.
21. Cohen, S., Dym, O., Albeck, S., Ben-Dov, E., Cahan, R., Firer, M., and Zaritsky, A. (2008) High resolution crystal of activated Cyt2Ba monomer from *Bacillus thuringiensis* subsp. *israelensis*. *J. Mol. Biol. 380*, 820–827.
22. Weng, Y.-P., Lin, Y.-P., Hsu, Ch-I., and Lin, J.-Y. (2004) Functional domains of a pore-forming cardiotoxic protein Volvatoxin A2. *J. Biol. Chem. 279*, 6805–6814.

23. Wu, D., and Federeci, B. A. (1993) A 20-kilodalton protein preserves cell viability and promotes CytA crystal formation during sporulation in *Bacillus thuringiensis*. *J. Bacteriol. 16*, 5276–5280.
24. Arantes, O., and Lereclus, D. (1991) Construction of cloning vectors for *Bacillus thuringiensis*. *Gene 108*, 115–119.
25. Wu, D., Johnson, J. J., and Federeci, B. A. (1994) Synergism of mosquitocidal toxicity between CytA and CryIV proteins using inclusions produced from cloned genes of *Bacillus thuringiensis* subsp. *israelensis*. *Mol. Microbiol. 13*, 965–972.
26. Muñóz-Garay, C., Portugal, L., Pardo-López, L., Jiménez-Juárez, N., Arenas, I., Gómez, I., Sánchez-López, R., Arroyo, R., Holzenburg, A., Savva, Ch. G., Soberón, M., and Bravo, A. (2009) Characterization of the mechanism of action of the genetically modified Cry1AbMod toxin that is active against Cry1Ab-resistant insects. *Biochim. Biophys. Acta 1788*, 2229–2237.
27. Thomas, W. E., and Ellar, D. J. (1983) *Bacillus thuringiensis* var. *israelensis* crystal δ-endotoxin: Effects on insect and mammalian cells *in vitro* and *in vivo*. *J. Cell Sci. 60*, 181–197.
28. Schägger, H., and von Jagow, G. (1987) Tricine-sodium dodecyl sulphate-polyacrylamide gel electrophoresis for the separation of proteins in the range from 1 to 100 kDa. *Anal. Biochem. 166*, 368–379.
29. Macek, P., Sendicic, L., and Lebez, D. (1982) Isolation and partial characterization of three lethal and hemolytic toxins from the sea anemone *Actinia cari*. *Toxicon 20*, 181–185.
30. Finney, D. (1971) in Probit analysis, pp 50−80, Cambridge University Press, New York.
31. Rausell, C., García-Robles, I., Sánchez, J., Muñoz-Garay, C., Martínez-Ramírez, A. C., Real, M. D., and Bravo, A. (2004) Role of toxin activation on binding and pore formation activity of the *Bacillus thuringiensis* Cry3 toxins in membranes of *Leptinotarsa decemlineata* [Say]. *Biochim. Biophys Acta 1660*, 99–105.
32. Chow, E., Singh, G. J. P., and Gill, S. S. (1993) Binding and aggregation of the 25 kDa toxin of *Bacillus thuringiensis* subsp. *israelensis* to cell membranes and alteration by monoclonal antibodies and amino acid modifiers. *Appl. Environ. Microbiol. 55*, 2779–2788.
33. Maceva, S. D., Puztai-Carey, M., Russo, P. S., and Butko, P. (2005) A detergent-like mechanisms of action of the cytolytic toxin Cyt1A from *Bacillus thuringiensis* var. *israelensis*. *Biochemistry 44*, 589–597.
34. Du, J., Knowles, B. H., Li, J., and Ellar, D. J. (1999) Biochemical characterization of *Bacillus thuringiensis* cytolytic toxins in association with phospholipid bilayer. *Biochem. J. 338*, 185–193.
35. Promdonkoy, B., and Ellar, D. J. (2003) Investigation of the pore forming mechanism of cytolitic δ-endotoxin from *Bacillus thuringiensis*. *Biochem. J. 374*, 255–259.
36. Promdonkoy, B., Rungrod, A., Promdonkoy, P., Pathaichindachote, W., Krittanai, Ch., and Panyim, S. (2008) Amino acid substitutions in aA and aC of Cyt2Aa2 alter hemolytic activity and mosquitolarvicidal specificity. *J. Biotechnol. 133*, 287–293.